

GREEN SYNTHESIS OF IRON NANOPARTICLES USING *ARTOCARPUS HETEROPHYLLUS* LAM., (JACKFRUIT) PEEL EXTRACT AND THEIR APPLICATION IN PHOTOCATALYTIC DEGRADATION OF METHYL ORANGE DYE

Dr. E.V.Sheena¹, Thaneshwari.K.R², Dr. A.K. Rathna Kumari³

¹Assistant Professors, PG Department of Plant Biology & Plant Biotechnology,
Shrimathi Devkunvar Nanalai Bhatt Vaishnav College For Women, Chromepet.

²II PG, Department of Plant Biology & Plant Biotechnology,
Shrimathi Devkunvar Nanalai Bhatt Vaishnav College For Women, Chromepet.

³Associate Professors, PG Department of Plant Biology & Plant Biotechnology,
Shrimathi Devkunvar Nanalai Bhatt Vaishnav College For Women, Chromepet

Email: sheena.ev@sdbnvc.edu.in

ABSTRACT

The ecofriendly synthesis of iron oxide nanoparticles shows great promise due to its non-toxic nature and environmentally friendly characteristics. Iron nanoparticles was synthesized from Artocarpus heterophyllus (Jack fruit) peel extract. The synthesized iron nanoparticles was confirmed by characterization techniques using Fourier transform infrared spectroscopy (FTIR), X-Ray diffraction (XRD), and Scanning electron microscopy (SEM) techniques. Further, the efficacy of synthesised nanoparticles has been demonstrated in the degradation of pollutant dye Methyl orange. The experiment showed that iron nanoparticles exhibited excellent degradation activity with a high removal efficiency of 83%

KEYWORDS: *Iron oxide nanoparticles, Artocarpus heterophyllus (Jack fruit) peel extract, Photocatalytic activity, Methyl orange dye degradation.*

1. INTRODUCTION

Production of metallic nanoparticles utilizing plant extracts has emerged as a sustainable and cost-effective biological method (Monga et al, 2016). Nanoparticles hold significant importance due to their unique properties and wide range of applications in various fields including agriculture, medicine, industrial and environmental sectors. Iron nanoparticles are extremely useful due to their redox and adsorption properties (MdIshak & Kamarudin, 2019).The biological sources used for the green synthesis of nanoparticles contain biologically active compounds, such as enzymes, proteins, polyphenols, flavonoids, and terpenoids, which can act as catalyzing, reducing, stabilizing, or capping agents for one-step synthesis.

Large quantities of fruit and vegetable waste are being discarded without full utilization, resulting in unhygienic environmental conditions. Therefore, effectively managing this waste is a critical issue that requires urgent attention. This study aims to utilize jackfruit peel waste extract to synthesize nanoparticles for addressing environmental concerns. The release of organic dyes as waste from industrial effluents has become a significant environmental challenge. Each year, approximately 700 million kilograms of organic dyes are discharged into water streams, posing a serious threat to the living populations that depend on these water sources for their basic needs. This study proposes using jackfruit peel extract to produce nanoparticles as a potential solution for reducing the release of organic dyes into the environment and mitigating their harmful effects.

2. MATERIALS AND METHOD

2.1. Sample collection and treatment of jackfruit peel

The collected jackfruit peels were washed thoroughly dried and ground using a mortar and pestle. (Fig 1). To prepare the jackfruit peel extract, a method adapted from Shahwan *et al.* was followed. 6g of the dried peel powder was mixed with 100ml of distilled water and heated for 15 minutes until the aqueous extract solution changed color to a pale yellow. The aqueous extract was stored in the refrigerator for further studies

2.2. Preparation of Fe NPs using waste Jackfruit peel extract

To prepare FeNPs, a 1:1 volume ratio of a freshly prepared 0.1 M FeCl₃ solution and yellow-colored jackfruit peel (JFP) extract was mixed and observed for any change in color. The formation of intense black color confirms the synthesis iron nanoparticles (Fe NPs-JF). The black precipitate was carefully collected, crushed into a fine powder, and stored in an Eppendorf tube for further use.

2.3. Characterization of Fe NPs-JF

The synthesized FeNPs-JF was characterized using techniques such as Fourier Transform Infrared Spectroscopy (FTIR), X-ray Diffraction (XRD) and Scanning Electron Microscopy with Energy-Dispersive X-ray Spectroscopy (SEM-EDX).

2.3.1 UV-Vis Spectrophotometric analysis

Confirmation of FeNPs synthesis was done by measuring the absorbance of the reaction mixture in a range of wavelengths from 200 to 800 nm to find the absorbance peak by using uv-vis spectrophotometer (thermo scientific evolution 201).

2.3.2 Optimization of synthesized FeNPs

FeNPs have been reported to exhibit a dark black color in aqueous solution. The stability of FeNPs synthesized from the jackfruit peel extract and observed daily for 15 days.

2.3.3. Effect of temperature

The effects of different temperatures are considered by mixing 1 ml of jackfruit peel extract with 1 ml of FeCl₃ (pH 7.0). Incubated at different temperature as 4°C, 12°C, 32°C, 53°C for 24 hrs and its absorbance was measured using UV spectrophotometer with wavelength ranging from 300-700 nm (Ramakrishna et al, 2019).

2.3.4 Fourier transforms infrared spectroscopy (FTIR)

FTIR is a spectroscopic technique that detects changes in the total composition of biomolecules by analyzing their functional groups. FTIR measures the vibration and rotation of molecules exposed to infrared radiation at a specific wavelength, allowing it to identify structural differences in molecular binding and reveal details about molecular interactions. The functional groups that played important role in the synthesis of iron nanoparticles was identified by using FT-IR (400-4000 cm⁻¹ range) from Thermo Scientific and Bruker-Germany.

2.3.5 XRD analysis of FeNPs

X-ray diffraction is a versatile, non-destructive analytical method for identification and quantitative determination of various crystalline forms present in the sample. To prepare thin films of nanoparticles for XRD analysis, the nanoparticles are drop-casted onto a low-background substrate. Nanoparticle samples with the desired orientation are then placed on a goniometer, where several reflections are evaluated. However, a sample with a random orientation may only require a brief scan through a 2θ diffraction angle. XRD characterization of nanoparticles typically starts with identifying the phase of the sample material. The crystal type in the sample is determined through a search-match process, performed in regions where high-intensity peaks are observed.

2.3.6 Scanning electron microscopy

Scanning electron microscopy provides information about the size, shape, and morphology of a sample. It is particularly useful for examining the surface morphology of nanoparticles, as it detects scattered electrons from the surface of the particles. To ensure the removal of any impurities, the nanoparticles were washed thoroughly with ethanol before analysis. Due to their magnetic properties, the particles were formed into pellets and then coated with a 10-15 nm layer before being dried. SEM observations were conducted using fixed electron beam energy of 30 kV and a working distance of 11 mm.

2.4 Photocatalytic degradation of methyl orange (MO)

The photocatalytic evaluation of synthesized Fe NPs was studied under visible light irradiation for the degradation of Methyl orange dye. For each measurement, 2 mg of the photocatalyst was introduced into 0.5M/L of dye solution. For adsorption of nanoparticles onto methyl orange, the mixture was stirred in the dark using magnetic stirrer. The suspension was then exposed to the sunlight, stirred continuously for hours using magnetic stirrer. During this process Aliquot were taken from solution at known time intervals. The degradation efficiency of the dye was studied using UV-visible spectroscopy at different conditions.

3. RESULTS AND DISCUSSION

The synthesized iron nanoparticle was identified using the following analytical techniques:

3.1 Uv-vis spectroscopy

Preliminary confirmation of the synthesized FeNPs was achieved by adding an iron salt solution to *Artocarpus heterophyllus* peel extract, resulting in a characteristic color change from yellow to dark black (Fig :2). The solution's absorbance spectra were then recorded across a wavelength range of 200-1000 nm. Highest absorption peak of the synthesized FeNPs was exhibited at volume ratio of 1:1. The high SPR observed may be due to the larger particle sizes in comparison to other ratios. Haiss *et al* (2007). The formation of Fe NPs was confirmed by the observation of maximum absorbance at a wavelength range of 380-620nm. (Fig: 3)

3.2. Effect of time

The stability of synthesized Fe NPs was checked at every 24 hrs. The result revealed that maximum stability was observed at 72 Hrs. at wavelength 517nm (Fig: 4). The stability of the synthesized FeNPs was tested in different temperature (4°C, 12°C, 32°C, 53°C). 3 ml of FeNPs and FeCl₃ was maintained at different temperature and after 24 hrs, its absorbance was measured using UV spectrophotometer with wavelength ranging from 524-534nm. Effect of temperature shown in different temperature in (Fig: 5 & 6) & Table 1

3.3 The Fourier transform infrared (FTIR) Spectroscopy

FTIR analysis identifies the potential functionalities present in extract which were responsible for carbon signature found in EDX. Several peaks were observed in the range 1000–3400 cm⁻¹. As fig 7 the FTIR spectrum revealed a broad absorption band in the region 3000-3500 cm⁻¹ which is ascribed to O–H stretching vibrations of H-bonded polyphenols. Due to their strong antioxidant properties, these polyphenols reduce Fe (II) ions and subsequently adsorb onto the surface of the iron nanoparticles. This provides a protective layer covering the iron nanoparticles from exposure to atmospheric oxygen, thereby enhancing their shelf life. Hence, the spectral analysis

revealed that besides clinging on the surface of these particles, the polyphenols also form an integral component of iron nanoparticles. Weak band around 540 cm^{-1} due to Fe–O stretching vibrations confirm the formation of Fe_2O_3 .

The peaks observed in the FTIR spectrum at 2927.94 cm^{-1} indicate the presence of alkane and the peak at 1625.99 cm^{-1} and 1101.35 cm^{-1} confirms the presence of conjugated alkene, and secondary alcohol, respectively. This observation is in agreement with a previous study done by Aisida *et al.* (2020). The shift in peak position within the range of $400\text{--}4000\text{ cm}^{-1}$ confirms that these functional groups are present in compounds that bind to the surface of the iron oxide.

3.4 XRD analysis

The XRD spectrum (Fig 8) shows diffraction peaks at values of 24.16° , 35.12° , 36.63° , 40.63° , 49.97° , 57.08° , and 59.42° corresponding to the crystal planes of 012, 104, 110, 113, 024, 116 and 018, indicating the formation of $\alpha\text{-Fe}_2\text{O}_3$ nanoparticles. The intense and sharp peak revealed that Fe_2O_3 nanoparticles formed by the reduction method using jackfruit peel extract were crystalline in nature. The results are almost similar to the results obtained for iron oxide nanoparticles by other researchers (Ahmmad *et al.*, 2013).

3.5 Scanning electron microscopy (SEM)

The morphology, surface details, and elemental composition of the Fe NPs-JF were determined using SEM. SEM image (Fig 9) of Fe NPs revealed that the nanoparticles tend to agglomerate, forming irregular spherical particles on the surface. According to Feng and Lim (2007), the close contact between iron nanoparticles is due to their magnetic properties. Similarly, Ramgopal *et al.* (2011) reported nanoparticle aggregation using soap nut extract for silver ion reduction, possibly influenced by the presence of various polyphenols in the fruit extract, which can significantly affect the morphology and size of iron nanoparticles (Varma, 2011). The average size was found to be approximately 200–500 nm, which is considered acceptable. Therefore, FE-SEM was found to be a more reliable method for determining the size of the nanoparticles.

3.6 Photocatalytic degradation of methyloange (MO)

The iron nanoparticles were used as the heterogeneous Fenton-like oxidants for the degradation of MO in an aqueous solution (Figure 11). No significant activity was detected even after few hours during dye removal process. When the iron nanoparticles were used, Methyl orange degraded and the color vanished almost completely with 87% efficiency after 6 h. The spectral band of Methyl Orange shifted from 790 nm to 390 nm with the aqueous mixture of Iron nanoparticles (fig: 10). This change in the position of the absorption peak might be attributed Methyl Orange protonation and azonium ions formation. (Shahwan *et al.*, 2011). The catalytic role of Fe NPs in the Fenton like process is shown in Figure 10. The Methyl Orange was efficiently degraded within 6 h by iron nanoparticles. The synthesized Iron nanoparticles degraded 55% of the initial MO concentration during the first 3 h. Then reduction in color degradation continued at the fourth hour and no significant reduction occurred in the next 2 h.

4. REFERENCES

- Ahmad, H., Venugopal, K., Rajagopal, K., De Britto, S., Nandini, B., Pushpalatha, H.G., et al., 2020. Green Synthesis and Characterization of Zinc Oxide Nanoparticles Using *Eucalyptus globules* and Their Fungicidal Ability Against Pathogenic Fungi of Apple Orchards. *Biomolecules*, 10(3), 425
- Aisida SO, Ahmad I, Zhao T-K, Maaza M, Ezema FI., 2020. Calcination effect on the photoluminescence, optical, structural, and magnetic properties of polyvinyl alcohol doped ZnFe₂O₄ nanoparticles. *J Macro mol Sci Part B*. 59:295–308.
- Bhatia D., Sharma N.R., Singh J., Kanwar R.S. 2017. Biological methods for textile dye removal from wastewater: a review. *Crit. Rev. Environ. Sci. Technol.* 1836–1876.
- Feng, J., Lim, T.-T. 2007. Iron-mediated reduction rates and pathways of halogenated methanes with nanoscale Pd/Fe: analysis of linear free energy relationship, *Chemosphere* 66, 1765–1774.
- Hais, W., Nguyen, T.K., Aveyard, T.J., and Fernig, D.G. 2007. Determination of size and concentration of gold nanoparticles from U.V./vis spectra,” *Analytical Chemistry*, vol. 79, no.11, pp. 4215–4221.
- Lassoued A., Lassoued M.S., Dkhil B., Ammar S., Gadri A. 2018. Photocatalytic degradation of methylene blue dye by iron oxide (α -Fe₂O₃) nanoparticles under visible irradiation. *J. Mater. Sci. Mater. Electron.* 29:8142–8152.
- M. Yuan, X. Fu, J. Yu, Y. Xu, J. Huang, Q. Li, D. Sun, 2020. Green synthesized iron nanoparticles as highly efficient fenton-like catalyst for degradation of dyes, *Chemosphere* 261, 127618.
- MdIshak, NAI., Kamarudin, S., Timmiati, SN., 2019 Green synthesis of metal and metal oxide nanoparticles via plant extracts: an overview. *Materials Research Express*. 10.1088/2053-1591.
- Monga, Y., Kumar, P., Sharma, R K., Filip, J., Varma, RS., Zbořil, R., Gawande, MB. 2020. Sustainable Synthesis of Nanoscale Zerovalent Iron Particles for environmental remediation. *Chem Sus Chem* 13 (13), 3288-3305.
- NIAM, NIAM 2011 Handling of Agricultural Wastes in APMC, Research report National Institute of Agricultural Marketing, a government of India organization, Jaipur, India.
- Pratik R, Shalaka AC, Vrishali BM, Kamble PS. 2012. Effect of biosynthesized silver nanoparticles on *Staphylococcus aureus* biofilm quenching and prevention of biofilm formation. *Int J Pharm Biosci.*; 3:1.
- Ramakrishna S, Ramalingam M, Kumar TS, Soboyejo WO. 2019. *Biomaterials: A Nano Approach*. Boca Raton, Florida, USA: CRC Press.
- Ramakrishna S, Ramalingam M, Sampath Kumar TS, Soboyejo WO. 2010. *Biomaterials: A Nano Approach*. 1st ed. Boca Raton, Florida: CRC Press.
- Salata, O.V. 2004. Applications of Nanoparticles in Biology and Medicine. *Journal of Nano Biotechnology*, 2, 1-6. <https://doi.org/10.1186/1477-3155-2-3>
- Shahwan T., Sirriah S.A., Nairat M., Boyacı E., Eroğlu A.E., Scott T.B., Hallam K.R., 2011. Green synthesis of iron nanoparticles and their application as a Fenton-like catalyst for the degradation of aqueous cationic and anionic dyes. *Chem. Eng. J.* 172:258.



FIGURE1- DRIED AND POWDERED FRUIT PEEL FROM *ARTOCARPUS HETEROPHYLLUS*

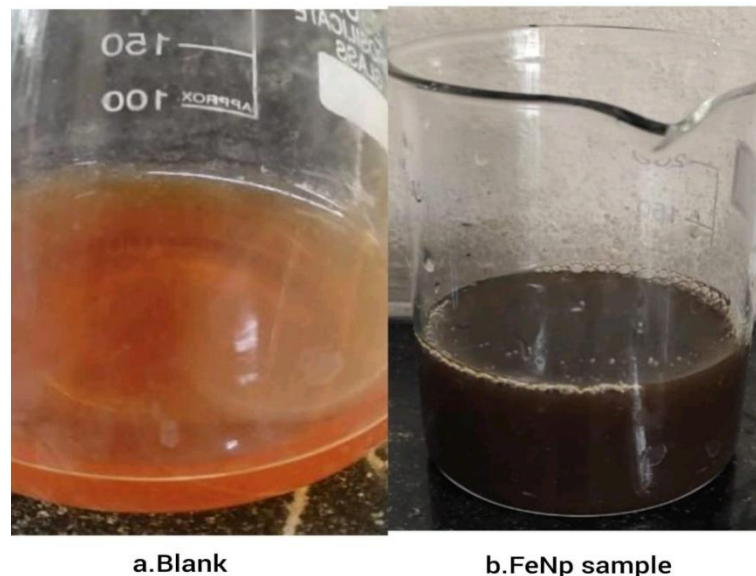


FIGURE2 - A) BLANK AND B) SAMPLE FOR UV VISIBLE SPECTROSCOPY FROM *ARTOCARPUS HETEROPHYLLUS* FRUIT PEEL

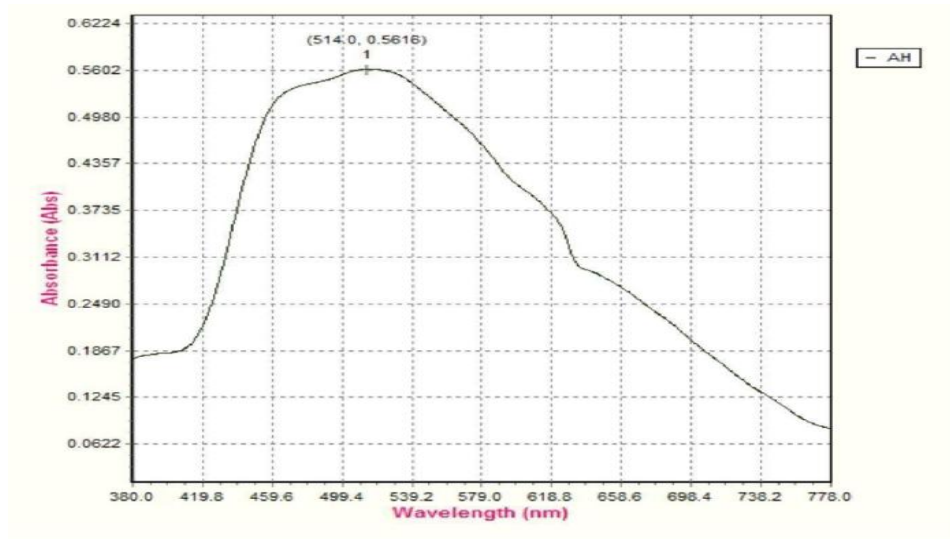


FIGURE 3- UV-VISIBLE SPECTRAL IMAGE FOR SYNTHESIZED FE NPS FROM *ARTOCARPUS HETEROPHYLLUS* PEEL EXTRACT

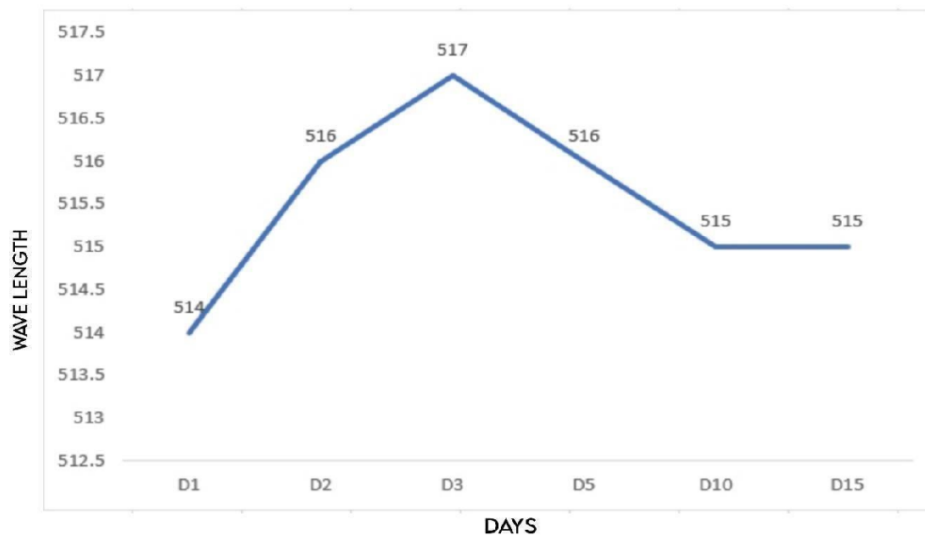


FIGURE 4- STABILITY TEST OF SYNTHESIZED FENPS FROM *ARTOCARPUS HETEROPHYLLUS* PEEL EXTRACT

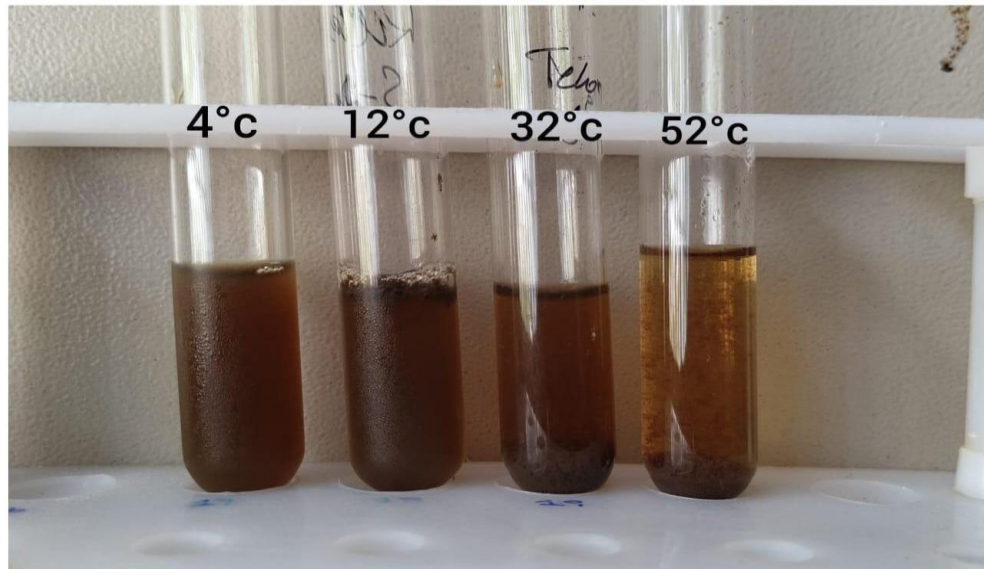


FIGURE 5 - STABILITY TEST FOR TEMPERATURE OF SYNTHESIZED FE NPS FROM *ARTOCARPUS HETEROPHYLLUS* PEEL EXTRACT

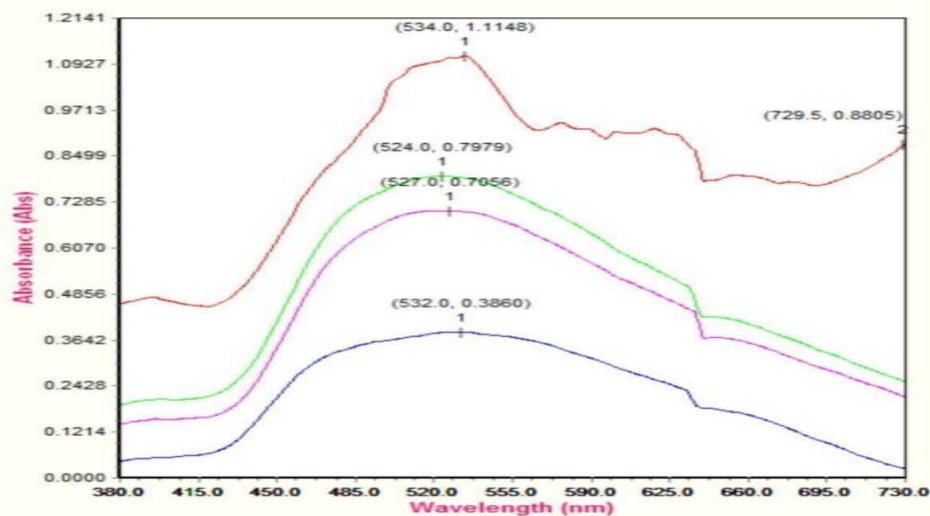


FIGURE 6- UV-VISIBL SPECTRAL IMAGE OF SYNTHESIZED FE NPS AT DIFFERENT TEMPERATURE FROM *ARTOCARPUS HETEROPHYLLUS* PEEL EXTRACT

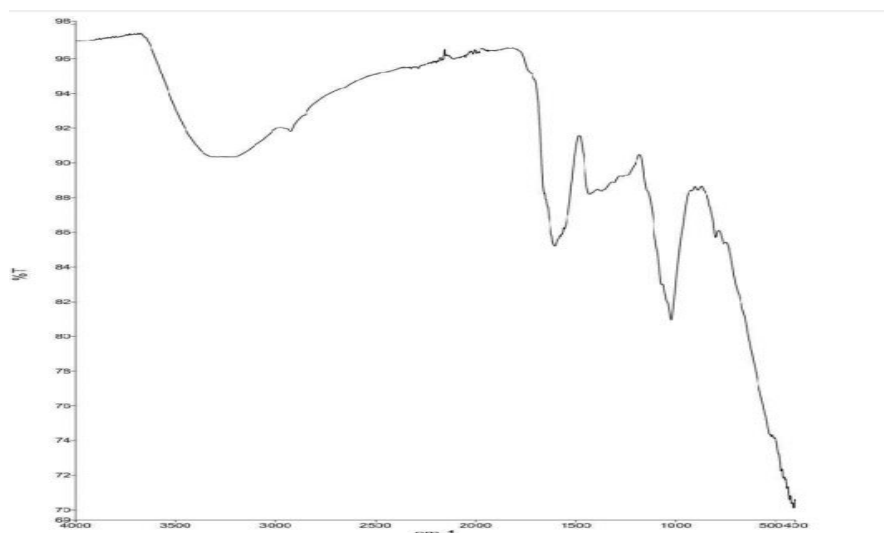


FIGURE 7 -FT-IR IMAGE OF SYNTHESIZED FE NPS FROM *ARTOCARPUS HETEROPHYLLUS* PEEL EXTRACT

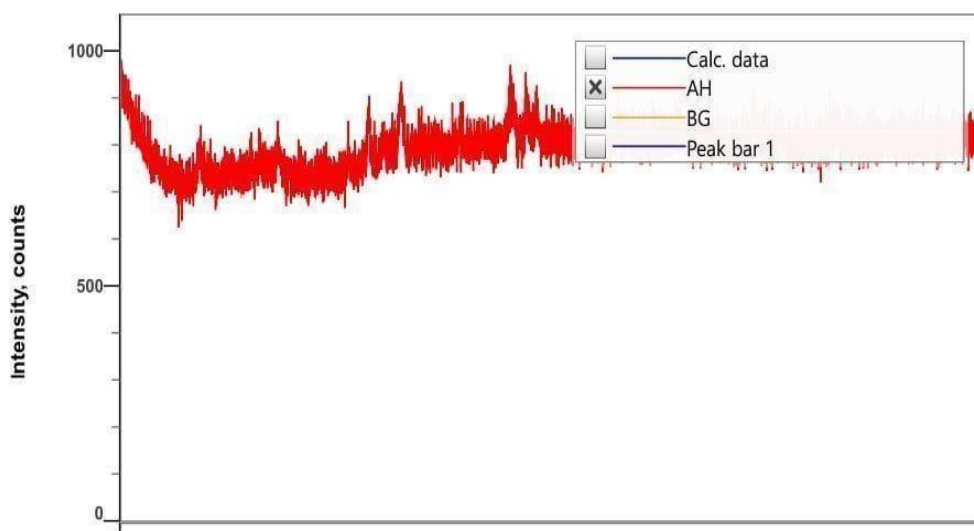


FIGURE 8-XRD SPECTRAL IMAGE OF SYNTHESIZED FENPS FROM *ARTOCARPUS HETEROPHYLLUS* PEEL EXTRACT

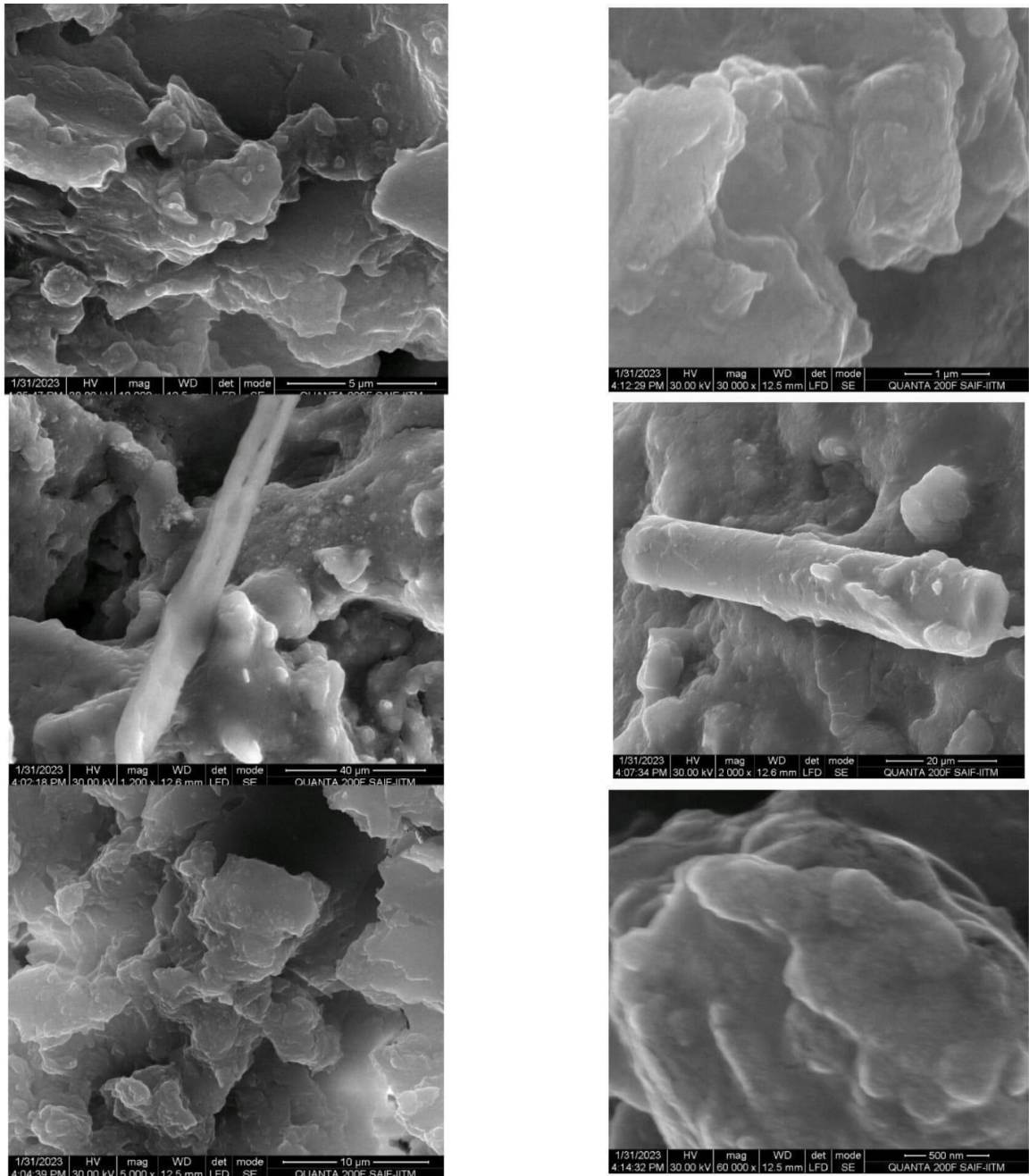


FIGURE 9-SEM IMAGE OF SYNTHESIZED FENPs FROM *ARTOCARPUS HETEROPHYLLUS* PEEL EXTRACT

TABLE1- VISUAL OBSERVATION AND UV-VIS ABSORPTION SPECTRA OF REACTION MIXTURES FOR SYNTHESIZED FENPS AT DIFFERENT TEMPERATURE

TEMPERATURE	NANOMETER
4 ⁰ C	524
12 ⁰ C	527
32 ⁰ C	532
52 ⁰ C	534

TABLE2 VISUAL OBSERVATION AND UV-VI SABSORPTION SPECTRA OF DYE DEGRADATION AT DIFFERENT TIME INTERVALS

DYE DEGRADATION	NANOMETER
1 hr	798
2 hr	616
3 hr	597
4 hr	556
5 hr	494
6 hr	388

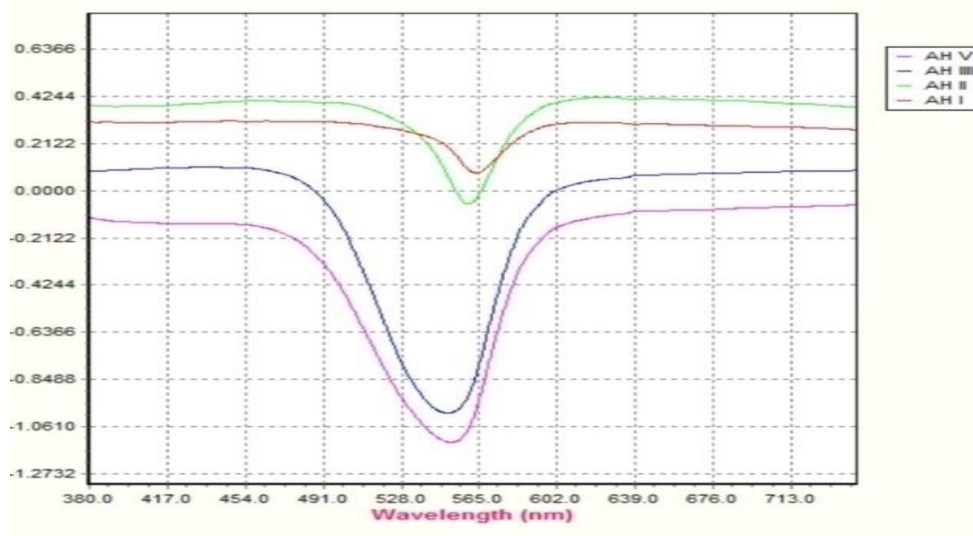
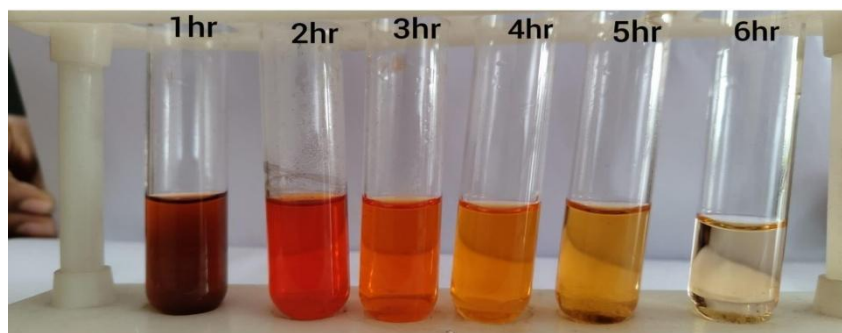


FIGURE 10- UV- VISIBLE SPECTRAL IMAGE OF DYE DEGRADATION FROM *ARTOCARPUS HETEROPHYLLUS* PEEL EXTRACT USING METHYL ORANGE



**FIGURE 11 –DEGRADATION OF METHYL ORANGE USING SYNTHESIZED FENPS FROM
ARTOCARPUS HETEROPHYLLUS PEEL EXTRACT**